Rapid Detection and Identification of Bacterial Strains By Fourier Transform Near-Infrared Spectroscopy

L. E. Rodriguez-Saona,† F. M. Khambaty,‡ F. S. Fry,‡ and E. M. Calvey*,‡

Joint Institute for Food Safety and Applied Nutrition (JIFSAN), Chemistry and Biochemistry Department, University of Maryland College Park, 200 C Street S.W., Washington, D.C. 20204, and U.S. Food and Drug Administration, 200 C Street S.W., Washington, D.C. 20204

The use of Fourier transform near-infrared (FT-NIR) spectroscopy and multivariate pattern recognition techniques for the rapid detection and identification of bacterial contamination in liquids was evaluated. The complex biochemical composition of bacteria yields FT-NIR vibrational transitions (overtone and combination bands) that can be used for classification and identification. Bacterial suspensions (*Escherichia coli* HB101, *E. coli* ATCC 43888, *E. coli* 1224, *Bacillus amyloliquifaciens*, *Pseudomonas aeruginosa*, *Bacillus cereus*, and *Listeria innocua*) were filtered to harvest the cells and eliminate the matrix, which has a strong NIR signal. FT-NIR measurements were done using a diffuse reflection-integrating sphere. Principal component analysis showed tight clustering of the bacterial strains at the information-rich spectral region of 6000−4000 cm^{-1}. The method reproducibly distinguished between different *E. coli* isolates and conclusively identified the relationship between a new isolate and one of the test species. This methodology may allow for the rapid assessment of potential bacterial contamination in liquids with minimal sample preparation.

Keywords: *FT-NIR spectroscopy; bacterial strains; PCA and classification*

INTRODUCTION

Fourier transform infrared (FT-IR) spectra of bacteria have shown highly specific patterns that may be unique for individual strains (*1*−*3*). FT-IR allows for the chemically based discrimination of intact microbial cells and produces complex biochemical fingerprints that are reproducible and distinct for different bacteria. The complex FT-IR spectra reflect the total biochemical composition of the microorganism, with bands due to major cellular constituents such as lipids, proteins, nucleic acids, polysaccharides, and phosphate-carrying compounds. Owing to the multitude of cellular components, broad and superimposed spectral bands are observed within the mid-IR region (4000−600 cm^{-1}) (*1*). Application of mathematical filter functions (first or second derivative) and the selection and combination of certain spectral windows and weighing factors accounting for specific contributions of cellular compounds have been used to enhance spectral resolution (*2*, *3*).

FT-IR has been applied for the microbiological classification and identification of *Enterobacteriaceae*, *Staphylococcus*, *Aeromonas*, *Pseudomonas*, *Streptococcus*, *Clostridium*, and *Legionella* strains (*2*−*4*), *Eubacterium* species (*5*), *Lactobacillus* (*6*), *Enterococcus* (*7*), and *Cyanobacteria* (*8*). Although FT-IR techniques have been used to discriminate between different bacteria taxa, occasionally down to the strain level, the potential of FT-near-infrared (FT-NIR) for the characterization of bacterial strains has not yet been investigated.

The NIR spectra of organic molecules are dominated by overtone and combination bands of fundamental vibrations involving highly anharmonic X−H (mainly C−H, N−H, and O−H) stretching modes. This technique provides fast and accurate measurements of chemical components, can be applied to small amounts of sample, is nondestructive (*9*), and gives information about structural and physical properties of materials (*10*, *11*). In addition, the NIR bands are 10−100 times less intense than the corresponding mid-infrared fundamental bands. This enables direct analysis of highly absorbing samples without extensive sample preparation (*12*, *13*). The use of Fourier transform technology in the NIR region has increased spectral reproducibility and wavenumber precision in comparison to results from dispersion instruments (*14*). The NIR region contains bands that often overlap, making it difficult to extract spectral parameters of the individual bands (*15*). Advances in chemometrics have provided a way of overcoming these problems by developing empirical models that relate the multiple spectral intensities from many calibration samples to the known analytes in these samples (*16*). Chemometric methods such as principal component analysis (PCA) and soft independent modeling by class analogy (SIMCA) have been extensively applied to the analysis of infrared spectra in a variety of areas within the fields of medicine, biology, forensic, and agricultural and food sciences (*7*). PCA is a well-known technique for the extraction and interpretation of systematic variance in multidimensional data sets by means of a small number of orthogonal variables (*17*, *28*). The concept is to remove the random variation (noise) and retain the principal components that capture the relevant variation. This analysis reveals if there are natural clusterings in the data and if there are outlier samples. It may also be possible to ascribe chemical (or biological or physical) meaning to the data patterns that emerge from PCA and to

* Author to whom correspondence should be addressed [telephone (202) 205-4716; fax (202) 260-1654; e-mail ecalvey@cfsan.fda.gov].

† JIFSAN.

‡ U.S. Food and Drug Administration.

10.1021/jf000776j CCC: $20.00
Published on Web 01/17/2001

estimate what portion of the measurement space is noise. PCA may be used in exploratory analysis to get graphical representations of similarities/differences in observations from multivariate data sets, including NIR spectral data.

The objectives of this study were to evaluate the feasibility of FT-NIR applications in microbiology and to develop methodology for the rapid identification of bacterial strains by combining FT-NIR spectroscopy with multivariate statistical methods.

MATERIALS AND METHODS

Strains and Growth Conditions. The following collection of bacterial strains was examined: *Escherichia coli* HB101, nonvirulent strain of *Escherichia coli* ATCC 43888, *Escherichia coli* 1224 (a nonpathogenic, wild-type food isolate), *Pseudomonas aeruginosa*, *Bacillus amyloliquifaciens*, *Bacillus cereus*, and *Listeria innocua*. Also included was a strain the identity of which was not revealed to the investigators until after the FT-NIR analyses were completed. The laboratory practices for handling the bacterial strains were conducted at the Biosafety Level 2 (*18*). Strains were grown aerobically overnight in 50 mL of brain heart infusion (BHI) broth at 37 °C with shaking at 110 rpm except for the *L. innocua*, which was not shaken. The optical density of 1:10 dilution of the bacterial suspensions in BHI broth was determined to estimate the cell numbers of these stationary phase cultures. The optical density was measured, and on the basis of empirical calculations, an aliquot of the cell suspension (containing a ~10 mg pellet) was transferred to microfuge tubes. The aliquot volume depended on the level of bacterial growth and usually was between 0.4 and 1.0 mL except for *Listeria*, which required ~4 mL. From each bacterial culture, four to five tubes were prepared to evaluate same-day reproducibility. For each set, the samples were filtered and dried within 30−34 h after inoculation. The reproducibility of cultures grown on different days was also examined. The tubes were centrifuged at 10000 rpm for 2 min, the supernatant was removed, and the resultant wet pellet was weighed and resuspended in 50 μL of sterile saline (0.9% NaCl) solution. The suspension was applied to a 0.2 μm pore size Anodisc membrane made of aluminum oxide (Whatman, Inc., Clifton, NJ) or a glass microfiber GF/C filter (Whatman, Inc.) to harvest the bacterial cells and eliminate the saline solution. Bacteria were analyzed directly by placing the membranes on the FT-NIR sapphire crystal. Spectral reproducibility was evaluated on replicated cultures.

Cell enumeration was done by the standard plate count (SPC) method. Ten milligrams of the wet bacterial pellet was resuspended in 1 mL of 0.9% NaCl solution, and serial dilutions were prepared. Aliquots (0.1 mL) of the 10^5-10^8 dilutions were plated (in duplicate) on BHI agar plates, and colonies were counted after the plates had been incubated at 35 °C for 24 h.

FT-NIR Measurements. All FT-NIR spectra were recorded using a Perkin-Elmer Spectrum Identicheck system operating at 8 cm^{-1} resolution. Measurements were made on filters (glass microfiber or Anodisc), by using the diffuse reflectance integrating sphere, equipped with a PbS detector. The filtration membrane, containing a dried film, was placed on the reflectance accessory for direct measurement by transflection using an aluminum diffuse reflector (Perkin-Elmer, Norwalk, CT). The reflector contained integral spacers that allow two passes of the beam through the sample to provide a total path length of 0.5 mm. The absorbance spectrum was obtained by ratioing the single-beam spectrum against that of the background, filter membrane. The FT-NIR spectra were recorded from 10000 to 4000 cm^{-1} at intervals of 4 cm^{-1}. Interferograms (128) were co-added followed by strong Beer−Norton apodization. The total number of data points was 1501 for each spectrum.

Multivariate Analyses. PCA was carried out by Pirouette pattern recognition software (version 2.51 for Windows NT, InfoMetrix, Inc., Woodinville, WA). The spectra were imported as JCAMP-DX files into the multivariate statistical program Pirouette 2.51, running on an IBM-compatible computer. The FT-NIR spectral data were mean-centered, area-normalized, and transformed to its second derivative based on a Savitzky−Golay polynomial filter. PCA was performed using the Nonlinear Iterative Partial Least Squares (NIPALS) algorithm. Outlier diagnostics were done by sample residual and Mahalanobis distance.

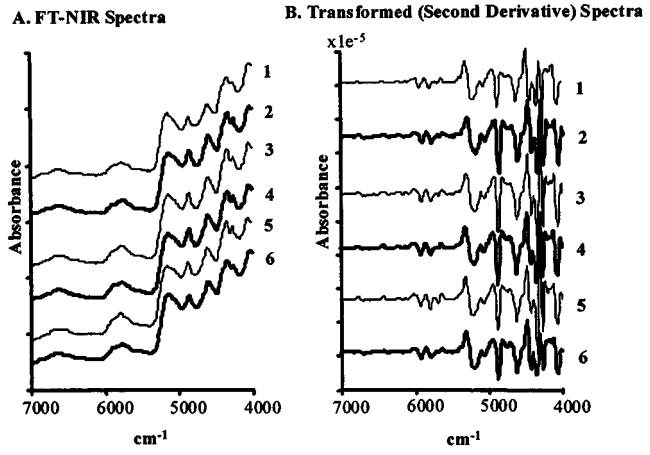

Figure 1. FT-NIR diffuse reflectance spectra (A) and second-derivative spectra (B) (21-point gap) of different bacterial strains: 1, *L. innocua*; 2, *E. coli* HB101; 3, *E. coli* ATCC 43888; 4, *E. coli* 1224; 5, *P. aeruginosa*; 6, *B. cereus*. Measurements were made on Anodisc membranes containing the bacterial films.

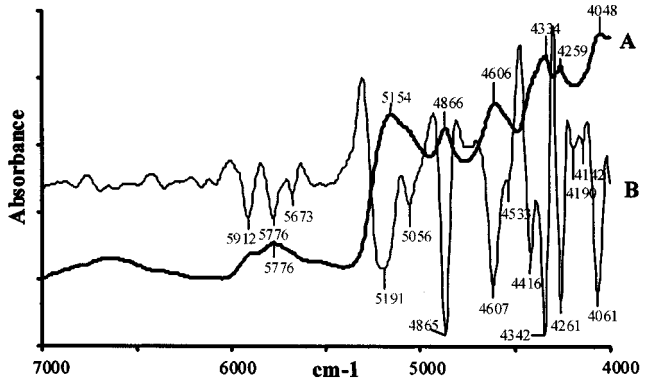

Figure 2. FT-NIR diffuse reflectance absorption spectra of *E. coli* HB101: (A) raw spectrum; (B) second-dervative (21-point gap) spectrum.

RESULTS AND DISCUSSION

FT-NIR Spectra of Bacterial Strains. Figure 1 shows the characteristic absorption spectra of the different bacteria evaluated. As the bacterial strains showed similar basic FT-NIR spectral patterns (Figure 1A), mathematical transformations were required to use the FT-NIR data for qualitative analysis. Second-derivative transformation (Figure 1B) of spectra extracted and highlighted distinct features among the bacterial strains, especially in the information-rich region of 6000−4000 cm^{-1}. Furthermore, derivative transformations removed baseline shifts, helping to reduce the variability between replicates (*8*). Using the Savitzky−Golay second derivative (optimal window size was 21 points) allowed the extraction of useful band information and reduced spectral noise (*19*, *29*).

The raw and derivatized FT-NIR spectrum of *E. coli* HB101 (Figure 2) was used to emphasize the major

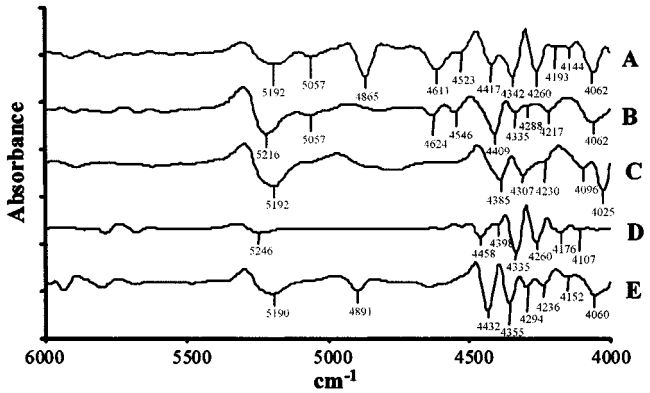

Figure 3. Second-derivative (21-point gap) spectra of (A) *P. aeruginosa*, (B) deoxyribonucleic acid standard, (C) glycogen standard, (D) lecithin standard, and (E) *N*-acetylmuramic acid standard.

absorption bands associated with the bacterial samples. The interpretation of the complex NIR spectra of bacterial cells is difficult because the diverse array of chemical compounds present can result in band overlapping, and a specific band in the spectra could be a composite of many bands containing information on more than one type of molecular vibration. The NIR absorbances for various generic functional groups (*12*) may be correlated to major cell constituents. FT-IR band assignments that have been tentatively assigned to chemical functional groups present in whole cells and macromolecules can be used to interpret the specific FT-NIR absorption bands generated by the bacterial cellular compounds (*2*−*4*, *8*). Also, FT-NIR spectra of selected standards of cellular components were measured (Figure 3) and analyzed to demonstrate correlation to some of the bands observed in bacterial spectra. The bands at 5912, 5776, and 5673 cm^{-1} could be related to first overtones of the CH stretching modes of CH_3, CH_2, and aromatic CH groups (*20*). Aromatic (∼5950 cm^{-1}) and heterocyclic (6084 and 6161 cm^{-1} for p-Trp and p-His, respectively) CH overtone transitions have been shown to make distinctive contributions at higher energy than the aliphatic CH (5650−5920 cm^{-1}) overtones (*20*). The absorption band at 5192 cm^{-1} for the bacterial strains was similar to bands observed in glycogen (5194 cm^{-1}) and *N*-acetylmuramic acid (5190 cm^{-1}) standards, which can be associated with the OH stretching and HOH deformation modes of polysaccharides (*12*). Also, the OH combination band from water has been assigned at 5200 cm^{-1} (*21*) and could be overlapping the glycogen signal. The FT-NIR bacterial bands at 5056 and 4061 cm^{-1} also occur on the DNA standard and could be associated with NH stretch and C−N−C first overtone modes, respectively (*12*). The bands at 4866 and 4606 cm^{-1} appear to be associated with combination bands characteristic of amide groups in the protein region. The region from 4500 to 5000 cm^{-1} contains combinations involving the NH stretching modes, and bands near 4874 and 4584 cm^{-1} have been assigned to combinations of amide A/I and amide B/II, respectively (*20*). Robert et al. (*22*) reported that proteins (myoglobin, β-lactoglobulin, and β-casein) exhibited common peaks at 4866, 4608, and 4255 cm^{-1} attributed to combination bands of amide A/I, amide I/II, and CH stretch/CH deformation. Combinations involving methylene CH stretching modes dominate the 4000−4500 cm^{-1} region (*20*). Bands at 4342 and 4260 cm^{-1} contain spectral features associated with aliphatic CH stretching modes of lipids. The phospholipid standard (lecithin) showed major absorption bands at 4335 and 4260 cm^{-1}, and Tkachuk (*23*) reported characteristic NIR absorption signals for lipids at 5807, 5681, 4336, and 4269 cm^{-1}. Polysaccharides exhibit important NIR bands in the C−H combination region (*24*); however, none of the glycogen bands in the 4400−4100 cm^{-1} region matched those present in the bacterial spectra. Nevertheless, the *N*-acetylmuramic acid standard, a constituent of the peptidoglycan (murein) layer of bacterial cell membrane, showed absorption bands centered at 4432, 4355, 4152, and 4060 cm^{-1} that were close to those present in the bacterial samples. The signal of phosphodiester functional groups present in nucleic acids, phosphorylated proteins, and polyphosphate storage products in the cell, reported for the FT-IR discrimination of bacterial strains (*8*), could not be assigned probably due to the weak NIR absorption of the P═O stretching bond vibration.

Optimization of Sample Preparation for Identification of Bacteria by FT-NIR. NIR analysis of aqueous systems is difficult because of the interference from broad vibrational bands of water that overlap the spectral information of solutes (*25*), which usually cannot be deconvoluted into their constituents. A filtration device (Millipore system) that uses filters to concentrate the bacterial cells and eliminate the effect of the matrix was evaluated for the rapid analysis of bacterial contamination in liquids instead of the standard technique that involves the use of mild vacuum-drying of resuspended bacterial colonies (in distilled water or saline solution) onto different optical plates that has been reported for FT-IR spectroscopy (*2*, *3*, *7*, *8*). The bacterial cells were trapped on the filter, the solvent was eliminated, and a homogeneous dried film was obtained. Polycarbonate and microporous polyethylene filters were deemed to be unsuitable because of their strong NIR absorption bands between 6000 and 4000 cm^{-1}, which concealed most of the bacterial spectral information. Fiberglass filters and Anodisc membranes considerably reduced the background interference, hence allowing the NIR spectral differences among bacterial strains to become prominent.

Initially, bacterial suspensions (5 mL) containing different cell concentrations [10^7−10^{10} colony-forming units (CFU)/mL] were filtered through a 25 mm diameter glass microfiber paper or Anodisc membrane. The filtration technique generated consistent FT-NIR spectral patterns for the different strains and showed potential for discrimination among bacterial strains. However, acceptable FT-NIR spectra were obtained only at the higher cell levels because the bacterial cells were spread onto an area much larger than the optical beam path of the reflectance accessory (15 mm diameter) and thus resulted in material that was not being used for the analysis. Sedimentation of the cells, resuspension of the pellet in 50 μL of saline solution, and application of the suspension on 13 mm diameter filters allowed the formation of films with an area similar to that of the reflectance beam path accessory. This procedure required less cell mass and yielded a reproducible film of bacteria with increased FT-NIR band intensities.

Differentiation of Bacterial Strains. Differentiation of the bacterial strains was performed using a mean-centered PCA on the derivatized spectra. A data set of 75 (glass microfiber) and 115 (Anodisc) spectra representing six bacterial taxa was analyzed. The data comprised repeated observations on cells collected from

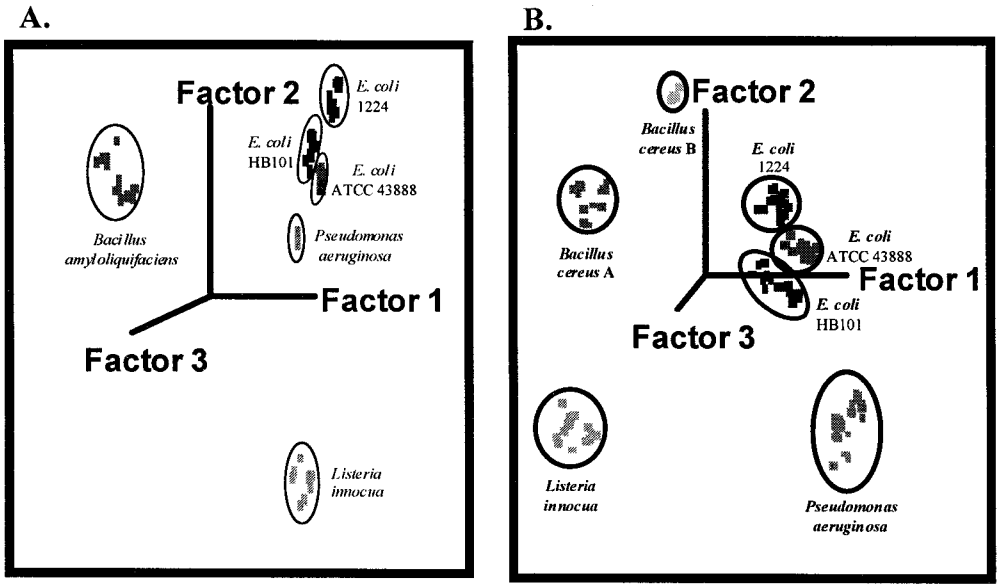

Figure 4. PCA of transformed (second-derivative, 21-point window) FT-NIR spectra bacterial strains (A) embedded on glass microfiber filters and (B) retained on the Anodisc membrane surface. The data comprised repeated observations on cells collected from a single stationary phase culture (four to five measurements) and also from cultures grown on subsequent days (replication). Data were collected in the 7000−4000 cm^{-1} spectral region.

a single stationary phase culture (four to five measurements) and also from cultures grown on subsequent days (replication). The scores plot, a projection of the original data onto the principal components, allowed the visualization of clustering among samples (sample patterns, groupings, or outliers). The FT-NIR spectral regions from 5600 to 5200 cm^{-1} were primarily affected by the changes in moisture content of the bacterial samples. Changes in the residual moisture content of samples could interfere with the NIR models (*26*), and removal of the bands that were influenced by the moisture absorbances from the PCA model improved the bacterial classification. PCA scores grouped the FT-NIR spectral information from bacteria retained on glass microfiber filters (Figure 4A) and Anodisc membranes (Figure 4B) into separate clusters. Gram-negative (*E. coli* and *Pseudomonas*) bacterial clusters were grouped more closely together, possibly due to similar fatty acid profiles in the outer membrane. The technique was able to discriminate among closely related *E. coli* strains. The reproducibility of the method was demonstrated by the tight clustering of specific bacterial samples analyzed as replicates on the same day and also when repeated on subsequent days.

Although FT-NIR measurements on bacteria retained on glass microfiber filters and Anodisc membranes showed potential for discrimination among bacterial strains, the distinct properties of the filters had an important effect on the amount of material required to obtain reproducible FT-NIR spectra. Anodisc membranes (surface filter) provided a smooth and flat surface for the retention of the bacterial cells, allowing the formation of a thin homogeneous film. However, the porous nature of glass microfiber filters (depth medium of intertwined fibers) required the use of higher levels of cell material to obtain reliable spectral data. Further experiments were focused on the use of Anodisc membranes to create reproducible films that give distinctive fingerprints in the FT-NIR region and allowed reducing the levels of cell material applied to the membrane. A problem experienced with the use of the Anodisc membranes was that the bacterial film peeled off, especially for the *E. coli* strains; this complicated the sample handling and increased the noise of the FT-NIR spectra (data not shown) due to changes in the physical properties of the material (the film usually cracked into many pieces). The peeling of the dried film can be avoided by applying less cell material (~10 mg) to the membranes.

Table 1. Average Cell Concentration of Bacterial Strains Used for FT-NIR Spectral Collection

bacterial strain	standard plate count (CFU/mg)
E. coli HB101	1.2×10^8
E. coli ATCC 43888	2.9×10^8
E. coli 1224	3.1×10^8
P. aureginosa	3.6×10^8
B. cereus	7×10^7
L. inoccua	5.2×10^8

A critical factor for the success of FT-NIR and multivariate techniques for bacterial characterization was the concentration of cell material applied to the membrane. Although the spectral data were normalized to compensate for changes in material concentration, it appears that differences in spectral features due to concentration (the more cell material, the richer the spectral information that is obtained) affected the PCA modeling. Therefore, the method required standardization of the amount of cell mass being applied to the membrane. The use of optical density as an indirect measurement of cell concentration in the suspensions reduced the FT-NIR intersample variability. However, the use of a resuspended pellet of wet bacterial cells gave a more reproducible film thickness and therefore was chosen to standardize the methodology. Approximately 10 mg of wet cell weight was used for our analysis, and the PCA analysis showed good clustering of the data (Figure 4B). The cell levels (cells per milligram) estimated by standard plate count method are shown in Table 1. A cell concentration between 10^8 and 10^9 CFU (<1 mL of bacterial suspension) deposited on the membranes gave the most reproducible spectra. Because NIR band intensities are usually 10−100 times weaker than the corresponding mid-IR fundamental bands (*27*), these results compared well with cell levels

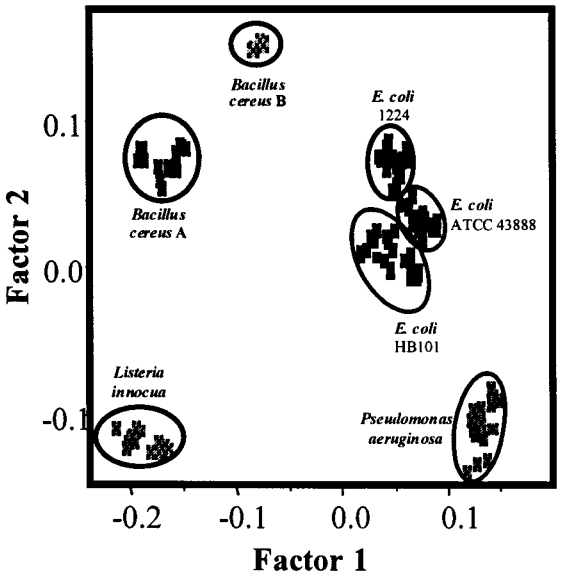

Figure 5. PC1 versus PC2 scores plot of FT-NIR spectra collected using the second-derivative (21-point window), considering the region from 7000 to 4000 cm^{-1}.

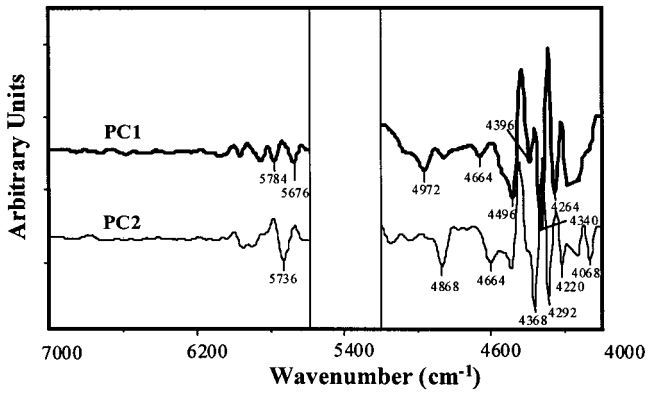

Figure 6. Loadings plot showing PC1 and PC2, accounting for 57 and 26% of the total variability. The spectral region from 5600 to 5200 cm^{-1} was excluded to minimize the effect of sample-to-sample differences in moisture content (OH combination broad band at 5200 cm^{-1}) of the cell material.

of 10^6-10^7 CFU reported for mid-IR bacterial discrimination (*7*, *8*). However, the fact that most bacteria can be trapped on membranes with a pore size of ≤ 0.2 μm allows the filtration of a large volume (i.e., 1 L) to concentrate the cells. This increases the sensitivity of the procedure and permits the reproducible detection of bacteria at levels 3-fold below those obtainable without filtering. The filtration technique also allows the removal of other interfering compounds (sugars, organic acids, etc.) present in the liquid matrix. Furthermore, the amount of cell material used for these experiments was near the upper limit of concentration that would not result in peeling of the bacterial film; this produced the strongest FT-NIR signal necessary for refinement of the technique. Studies to determine limits of detection (i.e., the smallest amount of cell material needed for reliable data) are being conducted.

To test the FT-NIR and multivariate techniques, a blind sample was included in the analysis. The PCA analysis located the test isolate close to the cluster of data points of the *B. cereus*, but it was clearly classified as unique (Figure 4B). The test isolate was later identified by traditional microbiological methods as another *B. cereus* strain. Although the *B. cereus* strains were taxonomically similar, the FT-NIR technique correctly assigned them to separate clusters, showing the value of this method as a strain-specific discrimination tool.

The FT-NIR method allowed for direct measurements of the membranes containing the bacterial film, without drying of the samples on expensive optical crystals, and also minimized subsequent cleanup and disinfection steps. Also, FT-NIR measurements do not require purging of the sample compartment for removal of CO_2 and H_2O vapor.

The PCA explained 95% of the total variability using the first six principal components (PC), whereas PC1 and PC2 were particularly representative of the spectral information and accounted for 82% of the total variance. The scores plot of PC1 versus PC2 displayed distinct clustering for the bacterial strains (Figure 5). Examination of the loading weights (Figure 6) indicated which FT-NIR frequencies contribute significantly to the variation in the data set. The glycogen absorption band at 5192 cm^{-1} was overlapped by the broad absorption of water (5200 cm^{-1}) and could not be resolved sufficiently by the second-derivative transformation to avoid interference from O−H vibrations of water and had to be excluded from the PCA model.

Differences in the major cellular constituents of bacteria are responsible for the unique and reproducible FT-NIR spectral patterns that allow chemometrics (PCA) to satisfactorily group the bacterial strains. Differences in cellular composition have been used to separate bacteria into Gram-positive and Gram-negative groups. Major components of the cell wall include a peptidoglycan (murein) layer, lipoproteins, phospholipids, proteins, and lipopolysaccharides and could play an important role in FT-NIR bacterial classification. The loadings showed sharp bands at the 4000−4500 cm^{-1} spectral region suggesting that the aliphatic CH and methylene stretching modes largely influenced the bacterial spectral variation (*20*). The loading plot also showed that bands in the regions from 4500 to 5000 cm^{-1} and from 5600 to 6100 cm^{-1} related to frequencies of amide band combinations and CH first overtones of methylene and aromatic/heterocyclic groups, respectively (*20*) contributed to the bacterial variance.

Conclusions. The use of FT-NIR spectral information and multivariate techniques showed potential for the identification and subtyping of different bacterial species. Transformation of the spectra by second derivatives resolved specific FT-NIR features in the 7000−4000 cm^{-1} region to allow PCA to reproducibly group the samples into different clusters. The development of a simple membrane-based procedure to produce a thin bacterial film resulted in increased sensitivity and allowed rapid discrimination among closely related strains. This methodology can be applied for monitoring bacterial contamination in liquid systems and may become a powerful tool for monitoring the safety of our food supply. The limits of sensitivity of this method need to be determined. Because this method does not require culturing the bacteria or amplifying specific genes, it can serve as a rapid screen for liquids in which potential contamination may exist. The generation of a library of major foodborne pathogens and the evaluation of more powerful multivariate classification methods (SIMCA or artificial neural networks) are needed for this approach to become a standard typing tool.

LITERATURE CITED

(1) Naumann, D.; Helm, D.; Labischinski, H. Microbiological characterizations by FT-IR spectroscopy. *Nature* **1991**, *351*, 81−82.

(2) Helm, D.; Labischinski, H.; Naumann, D. Elaboration of a procedure for identification of bacteria using Fourier transform IR spectral libraries: a stepwise correlation approach. *J. Microbiol. Methods* **1991**, *14*, 127−142.

(3) Helm, D.; Labischinski, H.; Schallehn G.; Naumann, D. Classification and identification of bacteria by Fourier transform infrared spctroscopy. *J. Gen. Microbiol*. **1991**, *137*, 69−79.

(4) Van der Mei, H. C.; Naumann, D.; Busscher, H. J. Grouping of oral streptococcal species using Fourier transform infrared spectroscopy in comparison with classical microbiological identification. *Arch. Oral Biol.* **1993**, *38*, 1013−1019.

(5) Alsberg, B. K.; Wade, W. G.; Goodacre, R. Chemometric analysis of diffuse reflectance-absorbance Fourier transform infrared spectra using rule induction methods: Application to the classification of *Eubacterium* species. *Appl. Spectrosc.* **1998**, *52*, 823−832.

(6) Curk, M. C.; Peladan, F.; Hubert, J. C. Fourier transform infrared (FTIR) spectroscopy for identifying *Lactobacillus* species. *FEMS Microbiol. Lett.* **1994**, *123*, 241−248.

(7) Goodacre, R.; Timmins, E. M.; Burton, R.; Kaderbhai, N.; Woodward, A. M.; Kell, D. B.; Rooney, P. J. Rapid identification of urinary tract infection bacteria using hyperspectral whole-organism fingerprinting and artificial neural networks. *Microbiology* **1998**, *144*, 1157−1170.

(8) Kansiz, M.; Heraud, P.; Wood, B.; Burden, F.; Beardall, J.; McNaughton, D. Fourier transform infrared microspectroscopy and chemometrics as a tool for the discrimination of cyanobacterial strains. *Phytochemistry* **1999**, *52*, 407−417.

(9) Williams, P. C.; Norris, K. H. Qualitative applications of near-infrared reflectance spectroscopy. In *Near-Infrared Technology in the Agricultural and Food Industries*; Williams, P., Norris, K., Eds.; American Association of Cereal Chemists: St. Paul, MN, 1987.

(10) Millar, S.; Robert, P.; Devaux, M. F.; Guy, R. C. E.; Maris, P. Near-infrared spectroscopic measurements of structural changes in starch-containing extruded products. *Appl. Spectrosc.* **1996**, *50*, 1134−1139.

(11) Liu, Y.; Cho, R.; Sakurai, K.; Miura, T.; Ozaki, Y. Studies on spectra/structure correlations in near-infrared spectra of proteins and polypeptides. Part I. A marker for hydrogen bonds. *Appl. Spectrosc.* **1994**, *48*, 1249−1254.

(12) Shenk, J. S.; Workman, J. J.; Westerhaus, M. O. Application of NIR Spectroscopy to Agricultural Products. In *Handbook of Near-Infrared Analysis*; Burns, D., Ciurczak, E., Eds.; Dekker: New York, 1992.

(13) Hall, J. W.; McNeil, B.; Rollins, M. J.; Draper, I.; Thompson, B. G.; Macaloney, G. Near-Infrared spectroscopic determination of acetate, ammonium, biomass and glycerol in an industrial *Escherichia coli* fermentation. *Appl. Spectrosc.* **1996**, *50*, 102−108.

(14) McClure, W. F.; Maeda, H.; Dong, J.; Liu, Y.; Ozaki, Y. Two-Dimensional correlation of Fourier Transform Near-Infrared and Fourier Transform Raman spectra I: Mixtures of sugar and protein. *Appl. Spectrosc.* **1996**, *50*, 467−475.

(15) Czarnecki, M. A.; Liu, Y.; Ozaki, Y.; Suzuki, M.; Iwahashi, M. Potential of Fourier transform near-infrared spectroscopy in studies of the dissociation of fatty acids in the liquid phase. *Appl. Spectrosc.* **1993**, *47*, 2162−2171.

(16) Thomas, E. V.; Haaland, D. M. Comparison of multivariate calibration methods for quantitative spectral analysis. *Anal. Chem*. **1990**, *62*, 1091−1099.

(17) Martens, H.; Naes, T. Models for calibration. In *Multivariate Calibration*; Martens, H., Naes, T., Eds.; Wiley: Chichester, U.K., 1989; Chapter 3.

(18) Richmond, J. Y., McKinney, R. W., Eds. *Biosafety in Microbiological and Biomedical Laboratories*, 4th ed.; U.S. Department of Health and Human Services, Centers for Disease Control and Prevention and National Institutes of Health: Washington, DC, 1999.

(19) Archibald, D. D.; Kays, S. E.; Himmelsbach, D. S.; Barton, F. E., II Raman and NIR spectroscopic methods for determination of total dietary fiber in cereal foods: A comparative study. *Appl. Spectrosc.* **1998**, *52*, 22−31.

(20) Wang, J.; Sowa, M. G.; Ahmed, M. K.; Mantsch, H. H. Photoacoustic near-infrared investigation of homopolypeptides. *J. Phys. Chem*. **1994**, *98*, 4748−4755.

(21) Espinoza, L. H.; Lucas, D.; Littlejohn, D. Characterization of hazardous aqueous samples by near-IR spectroscopy. *Appl. Spectrosc.* **1999**, *53*, 97−102.

(22) Robert, P.; Devaux, M. F.; Mouhous, N.; Dufour, E. Monitoring the secondary structure of proteins by near-infrared spectroscopy. *Appl. Spectrosc.* **1999**, *53*, 226−232.

(23) Tkachuk, R. Analysis of whole grains by near-infrared reflectance. In *Near-Infrared Technology in the Agricultural and Food Industries*; Williams, P., Norris, K., Eds.; American Association of Cereal Chemists: St. Paul, MN, 1987.

(24) Osborne, B. G.; Fearn, T. Theory of near infrared spectrophotometry. In *Near Infrared Spectroscopy in Food Analysis*; Osborne, B. G., Fearn, T., Eds.; Longman Scientific and Technical: Essex, U.K., 1986.

(25) Fischer, W. B.; Eysel, H. H.; Nielsen, O. F.; Bertie, J. E. Corrections to the baseline distortions in the OH-stretch region of aqueous solutions. *Appl. Spectrosc.* **1994**, 107−112.

(26) Kays, S. E.; Windham, W. R.; Barton, F. E., II. Effect of cereal product residual moisture content on total dietary fiber determined by near-infrared reflectance spectroscopy. *J. Agric. Food Chem*. **1997**, *45*, 140−144.

(27) Ciurczak, E. W. Principles of near-infrared spectroscopy. In *Handbook of Near-Infrared Analysis*; Burns, D., Ciurczak, E., Eds.; Dekker: New York, 1992.

(28) Cowe, I. A.; McNicol, J. W. The use of principal components in the analysis of near-infrared spectra. *Appl. Spectrosc.* ***1985***, *39*, 257−266.

(29) Hrushka, W. R. Data analysis: wavelength selection methods. In *Near-Infrared Technology in the Agricultural and Food Industries*; Williams, P., Norris, K., Eds.; American Association of Cereal Chemists: St. Paul, MN, 1987.

Received for review June 27, 2000. Revised manuscript received November 9, 2000. Accepted November 13, 2000. This project was funded by the Technical Support Working Group through the Department of the Army with BFRC DAAD05-98-R0548. We express our appreciation to the Technical Support Working Group for sponsoring this research effort.

JF000776J